Eur J Nucl Med Mol Imaging (2011) 38:1132–1138
DOI 10.1007/s00259-011-1783-3

ORIGINAL ARTICLE

Vascular time-activity variation in patients undergoing ^{123}I-MIBG myocardial scintigraphy: implications for quantification of cardiac and mediastinal uptake

Hein J. Verberne · Derk O. Verschure · G. Aernout Somsen · Berthe L. F. van Eck-Smit · Arnold F. Jacobson

Received: 23 November 2010 / Accepted: 1 March 2011 / Published online: 2 April 2011

Abstract
Purpose For the quantification of cardiac ^{123}I-metaiodobenzylguanidine (MIBG) uptake, the mediastinum is commonly used as a reference region reflecting nonspecific background activity. However, variations in the quantity of vascular structures in the mediastinum and the rate of renal clearance of ^{123}I-MIBG from the blood pool may contribute to increased interindividual variation in uptake. This study examined the relationship between changes in heart (H) and mediastinal (M) counts and the change in vascular ^{123}I-MIBG activity, including the effect of renal function.
Methods Fifty-one subjects with ischemic heart disease underwent early (15 min) and late (4 h) anterior planar images of the chest following injection of ^{123}I-MIBG. Vascular ^{123}I-MIBG activity was determined from venous blood samples obtained at 2 min, 15 min, 35 min, and 4 h post-injection. From the vascular clearance curve of each subject, the mean blood counts/min per ml at the time of each acquisition and the slope of the clearance curve were determined. Renal function was expressed as the estimated creatinine clearance (e-CC) and the estimated glomerular filtration rate (e-GFR). Relations between H and M region of interest (ROI) counts/pixel, vascular activity, and renal function were then examined using linear regression.
Results Changes in ROI activity ratios between early and late planar images could not be explained by blood activity, the slope of the vascular clearance curves, or estimates of renal function. At most 3% of the variation in image counts could be explained by changes in vascular activity (p= 0.104). The e-CC and e-GFR could at best explain approximately 1.5% of the variation in the slopes of the vascular clearance curve (p=0.194).
Conclusion The change in measured H and M counts between early and late planar ^{123}I-MIBG images is unrelated to intravascular levels of the radiopharmaceutical. This suggests that changes in M counts are primarily due to decrease in soft tissue activity and scatter from the adjacent lungs.

Keywords ^{123}I-MIBG · Renal function · Quantification · Myocardial scintigraphy · Mediastinum

H. J. Verberne (✉) · D. O. Verschure · B. L. F. van Eck-Smit
Department of Nuclear Medicine, room F2-238, Academic Medical Center, University of Amsterdam,
PO Box 22700, 1100 DE, Amsterdam, The Netherlands
e-mail: h.j.verberne@amc.uva.nl

D. O. Verschure · G. A. Somsen
Department of Cardiology, Onze Lieve Vrouwe Gasthuis, Amsterdam, The Netherlands

G. A. Somsen
Cardiology Centers of the Netherlands, Amsterdam, The Netherlands

A. F. Jacobson
Cardiac Center of Excellence, GE Healthcare, Princeton, NJ, USA

Introduction

The myocardial sympathetic nervous system is activated in patients with heart failure (HF) and this activation has been shown to be associated with increased mortality [1]. Cardiac sympathetic hyperactivity can be scintigraphically visualized by ^{123}I-metaiodobenzylguanidine (MIBG), a radiolabeled analogue of noradrenalin. This noninvasive technique has been demonstrated to be a powerful prognostic marker in HF patients [2–4].

In myocardial ^{123}I-MIBG imaging, the most commonly used quantitative parameters are the heart to mediastinum (H/M) ratio and washout (WO) determined from planar images. The H/M is a measure of specific to nonspecific uptake, while the WO is a measure of neuronal integrity. A basic assumption associated with use of the mediastinum as a reference for H/M and WO calculations is that the counts in this region represent nonspecific binding of the radioligand.

One potential confounder for assessment of nonspecific ^{123}I-MIBG background activity is residual tracer in the blood. Since the mediastinum contains a relatively large volume of vascular structures, intravascular ^{123}I-MIBG activity may contribute to total mediastinal activity which may influence the quantification of the H/M ratio. Since the clearance rate of ^{123}I-MIBG from the blood is largely dependent on renal function [5, 6], and renal dysfunction is often present in HF patients, differences in the rate of vascular clearance may also contribute to increased inter-individual variation in uptake quantification [7, 8].

The objective of this study was to assess the magnitude of the influence of residual vascular ^{123}I-MIBG activity on image quantification by examining the relationship between changes in vascular activity and changes in heart (H) and mediastinal (M) activity between early and late planar ^{123}I-MIBG images.

Materials and methods

As part of a prospective multicenter trial [9], 51 subjects (48 male, 3 female; mean age 65.2) with ischemic heart disease (history of ≥ 1 myocardial infarction) underwent myocardial ^{123}I-MIBG imaging. The study protocol conformed to the ethical guidelines of the 1975 Declaration of Helsinki as reflected in a priori approval by each institution's human research committee. All subjects signed informed consent before performance of any study procedure.

Imaging procedures

All subjects received 370 MBq (10 mCi;±10%) of ^{123}I-MIBG (AdreView™, GE Healthcare) and underwent 10-min planar images of the anterior thorax at 15 min (early; e) and 4 h (late; l) post-injection (p.i.). The images were acquired with a 20% energy window centered at 159 keV, low-energy high-resolution (LEHR) collimation, and stored in a 128×

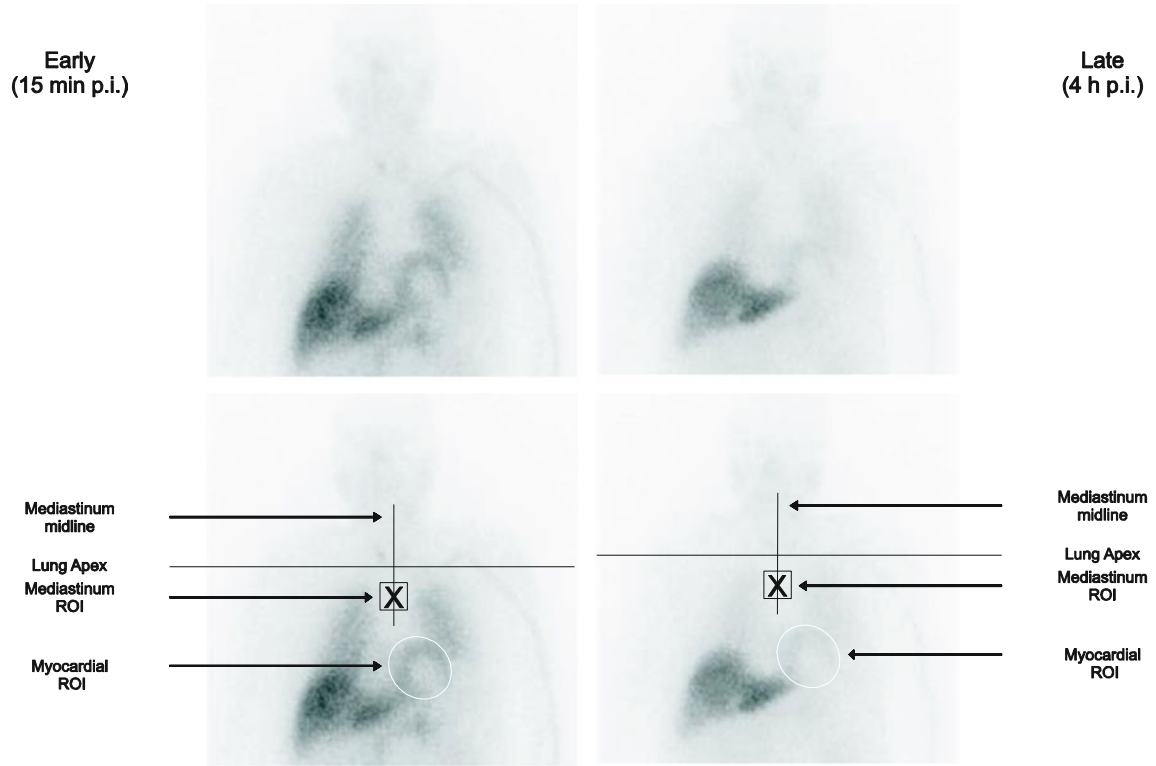

Fig. 1 The *upper panels* show an example of the planar ^{123}I-MIBG images of a male subject (age 58 years, NYHA III, LVEF 36%) with a history of a previous myocardial infarction. The *upper panel on the left* displays the image at 15 min p.i. (early) and the *upper panel on the right* shows the image at 4 h p.i. (late). The *lower panels* display the positioning of the ROIs on the early (*lower left*) and late (*lower right*) planar images. The positioning of the mediastinal ROI was standardized in relation to the lung apex and the midline between the lungs. In this example the early H/M was 1.54, the late H/M 1.40, and myocardial WO 9%

128 matrix. All digital image files were sent to an Imaging Core Laboratory (ICL) for evaluation and analysis.

Image analysis

An experienced nuclear medicine technologist processed all the planar images to determine the H and M count densities. The heart region of interest (ROI) was drawn manually to include both ventricles and any atrial activity that was clearly visible. A 7×7 pixel square mediastinal ROI was drawn in the upper mediastinum, using the apices of the lungs as anatomic landmarks (Fig. 1). Activity per ROI (mean counts/pixel) was corrected for decay to the time of injection and expressed as activity in the myocardium and mediastinum at 15 min and 4 h p.i. (H_e, H_l, H_l/H_e, M_e, M_l, and M_l/M_e). In addition, commonly used semiquantitative ^{123}I-MIBG myocardial parameters were assessed to better describe the clinical condition of the subjects. Early (15 min p.i.) and late (4 h p.i.) H/M ratios were calculated as the ratios of the mean counts per pixel in the two ROIs. All images and ROIs were reviewed by three independent readers, and a single aggregate H/M was derived for each image, either the value accepted by at least two readers, or if this criterion was not satisfied, the average H/M for all readers [9]. In addition, myocardial WO was calculated as:

$$\left\{\frac{(\text{early H/M} - \text{late H/M})}{\text{early H/M}}\right\} \times 100\%$$

Vascular activity

Blood samples (2 ml) were taken at 2 min, 15 min, 35 min, and 4 h p.i. Subsequently, 1-ml aliquots were counted in a well counter (energy peak at 159 keV with a 15% energy window). Activity (counts/min) was corrected for decay to the time of injection. For each patient a vascular clearance curve was plotted. Figure 2 shows a typical example with

Table 1 Demographic and cardiac medical history information for the 51 subjects included in the study

Baseline characteristics	
Male/female	48/3 (94/6%)
Age (years)	65.3±9.1 (42–84)
NYHA (I/II/III)	4/28/11 (8/55/22%)
ACC/AHA HF class (B/C)	15/36 (29/71%)
LVEF	33±8 (15–48)
Medication	
Beta-blockers	45 (88%)
ACE inhibitor/AT-II receptor blockers	46 (90%)
Aldactone	16 (32%)
Amiodarone	10 (20%)
Calcium channel blocker	12 (24%)
Estimates of renal function	
Creatinine (μmol/l)	113.4±42.4 (59–296)
e-CC (ml/min)	74.8±29.2 (19.9–156.9)
e-GFR (ml/min per 1.73m^2)	66.2±21.4 (19.1–125.6)
Semiquantitative ^{123}I-MIBG parameters	
Early H/M	1.51±0.25 (0.60–1.99)
Late H/M	1.44±0.18 (1.05–1.96)
Myocardial WO (%)	8.2±6.8 (5.3–10.8)

Data are expressed as mean ± SD and range or as absolute numbers and percentage

NYHA New York Heart Association functional classification, *LVEF* left ventricular ejection fraction, *ACC/AHA HF class* American College of Cardiology and American Heart Association classification of HF, *e-CC* estimated creatinine clearance calculated using the Cockcroft-Gault equation, *e-GFR* estimated glomerular filtration rate calculated using the abbreviated Modification of Diet in Renal Disease (MDRD) equation

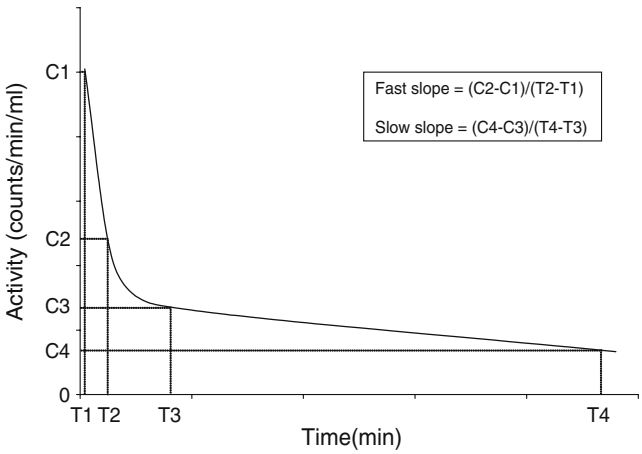

Fig. 2 In this typical example of a blood activity clearance curve, there is a clear distinction between a more accelerated phase and a slower phase. The slopes of both the faster (S_f) and slower (S_s) phases were calculated as illustrated in the figure

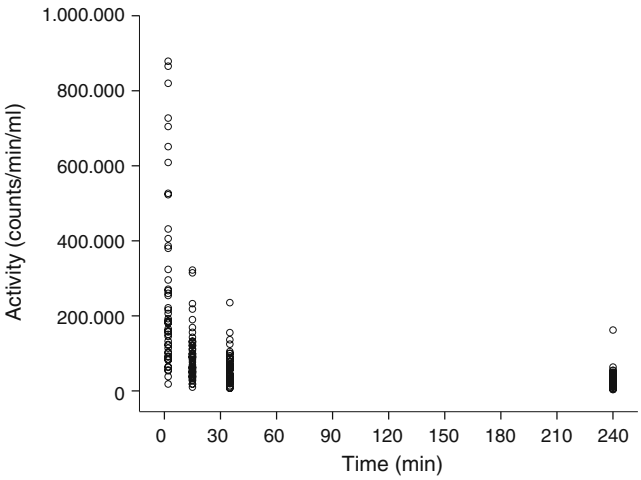

Fig. 3 Scatter plot showing the blood activity in relation to time for all subjects

Table 2 Slope of blood activity clearance curve (biexponential curve fitting)

	Fast part	Slow part	Ratio fast vs slow
Slope of clearance curve (counts/min)	−0.166±0.083 (−0.353 to −0.034)	−0.003±0.001 (−0.007 to −0.001)	63.11±45.00 (13.71–227.12)

Data are expressed as mean ± SD and range

two distinct phases, an accelerated clearance followed by a slower clearance. The slopes of the two phases of the clearance curves were determined according to biexponential curve fitting [accelerated phase (S_f) and the slower phase (S_s), expressed as cpm/ml per min].

Based upon the vascular clearance curve, the mean activity (cpm/ml) was calculated for the time intervals during which the two planar images were acquired (15–25 min and 3 h 50 min–4 h p.i.: V_e and V_l). The ratio of V_e and V_l and the ratio between the slopes of the accelerated phase (S_f) and the slower phase (S_s) of the blood clearance were then calculated.

Determination of renal function

Serum concentrations of creatinine were determined from blood samples obtained as part of screening evaluations performed within 7 days prior to ^{123}I-MIBG imaging. Analyses were performed at a central laboratory, with reference ranges of 75–111 μmol/l for men and 53–106 μmol/l for women.

Renal function was estimated using two methods. Estimated creatinine clearance (e-CC) was calculated (in ml/min) using the Cockcroft-Gault equation [10]:

$$e-CC=\frac{(140-[age\ (years)])\times[weight\ (kg)]}{[serum\ creatinine(\mu mol/L)]}\times(1.04\ for\ females\ and\ 1.23\ for\ males)$$

Estimated glomerular filtration rate (e-GFR) was calculated using the abbreviated Modification of Diet in Renal Disease (MDRD) equation [11]:

$$e-GFR=32788\times[serum\ creatinine\ (\mu mol/L)]^{-1.154}\times[age\ (years)]^{-0.203}\times[0.742\ for\ females]\times[1.212\ for\ blacks]$$

e-GFR was expressed per 1.73 m^2 of body surface area (ml/min per 1.73 m^2). According to the guidelines for identification, management, and referral of adults with chronic kidney disease, patients were stratified as having impaired kidney function [e-CC or e-GFR < 60 ml/min(per 1.73 m^2)] or normal function {e-CC or e-GFR [≥ 60 ml/min (per 1.73 m^2)]} [12].

Statistical analysis

Linear regression was used to examine the relationships between the vascular activity ratio (V_l/V_e), the slope of the vascular clearance curve (S_f/S_s), and the scintigraphically determined activity in the myocardium and mediastinum at 15 min and 4 h p.i. (H_e, H_l, H_l/H_e, M_e, M_l, and M_l/M_e). The overall goodness-of-fit was expressed as the adjusted R^2. The F test was used to assess whether the analysis explained a significant proportion of the variability. A $p<0.05$ was considered to indicate a statistically significant difference. A significant adjusted R^2 would indicate that variation in the scintigraphically determined parameters could be explained by a percentage (adjusted R^2) of change in vascular activity. All statistical analyses were performed with SPSS (SPSS for Windows, version 17.0.2, SPSS Inc., Chicago, IL, USA).

Results

Demographic and cardiac medical history information for the 51 subjects included in the study is summarized in Table 1. The majority of patients was male, had New York Heart Association (NYHA) class II HF, and had left ventricular ejection fraction (LVEF) < 40%. Eight patients had no history of HF. The majority of subjects were on a combination of beta-adrenergic receptor blockers and angiotensin-converting enzyme (ACE)

Table 3 Intravascular and imaging parameters

	Early (15 min)	Late (240 min)	Ratio late vs early
Intravascular activity (counts/min/ml)	93,379±65,841 (10,074–322,169)	31,702±23,298 (3,568–162,250)	0.35±0.11 (0.13–0.65)
Myocardial activity (counts/min)	97±41 (28–185)	61±27 (17–132)	0.63±0.08 (0.47–1.05)
Mediastinal activity (counts/min)	64±28 (21–115)	43±20 (13–82)	0.67±0.09 (0.48–1.15)

Data are expressed as mean ± SD and range

Table 4 Variability of scintigraphic parameters in relation to intravascular activity (linear regression)

	Constant	SE c	Coefficient b	SE b	Adjusted R^2	p value
M_e vs V_e	564.2	64.8	0.001	0.001	0.028	0.120
M_l vs V_l	430.2	45.8	0.001	0.001	0.001	0.905
M_l/M_e vs V_l/V_e	0.67	0.05	0.014	0.122	0.006	0.912
H_e vs V_e	878.4	97.3	0.001	0.001	0.014	0.191
H_l vs V_l	602.8	63.2	0.001	0.002	0.001	0.822
H_l/H_e vs V_l/V_e	0.59	0.04	0.126	0.109	0.01	0.253

SE standard error, M_e scintigraphically determined mediastinal counts 15 min p.i. (early), M_l scintigraphically determined mediastinal counts 4 h p.i. (late), H_e scintigraphically determined myocardial counts 15 min p.i. (early), H_l scintigraphically determined myocardial counts 4 h p.i. (late), V_e intravascular radioactivity 15 min p.i. (early), V_l intravascular radioactivity 4 h p.i. (late)

inhibitors or angiotensin II (AT-II) receptor blockers (Table 1).

Estimates of renal function showed a substantial variation (Table 1). In 26 (51%) patients creatinine levels were above the normal limit (25 men and 1 woman). Calculated e-CC was < 60 ml/min in 19 (38%) patients and the calculated e-GFR was < 60 ml/min per 1.73 m^2 in 24 (47%) patients.

There was a considerable range in the initial (i.e., fast) part of the ^{123}I-MIBG vascular clearance curves (Fig. 3). Despite this individual variation, the mean S_f was more than 60 times steeper compared to the mean S_s (Table 2). Mean intravascular activity (cpm/ml) decreased approximately 65% between 15 min and 4 h p.i. (Table 3). The mean scintigraphically determined myocardial and mediastinal activity (counts/min) decreased approximately 37 and 33%, respectively, between 15 min and 4 h p.i. (Table 3).

Variation in any of the scintigraphic parameters (M_e, M_l, M_l/M_e, H_e, H_l, and H_l/H_e) could not be explained by intravascular activity (Table 4). At most the counts in the blood at 15 min (V_e) could explain approximately 3% of the variation in the mediastinal counts at 15 min (M_e) (p= 0.120). Variation of the scintigraphic parameters could also not be explained by the slope of the clearance curves (Table 5). The slope of the clearance curves could at best explain up to 3% of the variation in the mediastinal counts (M_e vs S_f and M_l vs S_s, p=0.105 and p=0.100, respectively).

The variability in the change of intravascular activity (S_f, S_s, and S_f/S_s) could not be explained by either estimate of renal function (e-CC or e-GFR) (Table 6). The e-CC could at best explain approximately 1.5% of the variation in the fast slope of the vascular clearance curve (e-CC vs S_f, p=0.194).

Discussion

Most in vivo scintigraphic quantification of regional neurotransporter activity or receptor density involves comparison of uptake in a target ROI to that in a reference region of nonspecific uptake/binding. For assessment of sympathetic myocardial activity with ^{123}I-MIBG scintigraphy, use of the mediastinum as a reference region is based on the assumption that there is a negligible amount of specific uptake of ^{123}I-MIBG in this region. In addition, presence of ^{123}I-MIBG in the blood pool is also assumed to be insignificant. The present results demonstrate that changes in blood pool/vascular ^{123}I-MIBG activity do not significantly correlate with changes in heart and mediastinum activity between early and late planar images. This is

Table 5 Variability of scintigraphic parameters in relation to the slopes of the blood activity clearance curve (linear regression)

	Constant	SE c	Coefficient b	SE b	Adjusted R^2	p value
M_e vs S_f	532.9	83.3	−738.779	447.576	0.033	0.105
M_l vs S_s	542.0	69.4	33,361	19,957	0.032	0.100
M_l/M_e vs S_s/S_f	0.670	0.022	$4.44\ 10^{-5}$	0.022	0.001	0.875
H_e vs S_f	−0.127	0.031	$-3.99\ 10^{-7}$	−0.192	0.018	0.172
H_l vs S_s	0.004	0.000	$8.98\ 10^{-7}$	0.000	0.016	0.177
H_l/H_e vs S_s/S_f	0.631	0.020	$-2.21\ 10^{-7}$	0.000	0.001	0.999

SE standard error, M_e scintigraphically determined mediastinal counts 15 min p.i. (early), M_l scintigraphically determined mediastinal counts 4 h p.i. (late), H_e scintigraphically determined myocardial counts 15 min p.i. (early), H_l scintigraphically determined myocardial counts 4 h p.i. (late), S_f slope of the accelerated (fast: f) part of the blood activity clearance curve, S_s slope of the slower (s) part of blood activity clearance curve

Table 6 Variability of estimates of renal function in relation to the slopes of the blood activity clearance curve (linear regression)

	Constant	SE c	Coefficient b	SE b	Adjusted R^2	p value
e-CC vs S_f	62.9	8.4	−59.3	45.1	0.014	0.194
e-CC vs S_s	63.6	10.3	−3,470.1	2,953.7	0.007	0.245
e-CC vs S_f/S_s	69.9	6.5	0.052	0.084	−0.012	0.536
e-GFR vs S_f	63.5	6.3	−11.0	33.8	−0.017	0.746
e-GFR vs S_s	63.2	7.6	−947.9	2,158.8	−0.015	0.666
e-GFR vs S_f/S_s	65.4	4.8	−0.002	0.62	−0.019	0.970

SE standard error, *e-CC* estimated creatinine clearance based on Cockcroft-Gault equation, *e-GFR* estimated glomerular filtration rate according to the abbreviated Modification of Diet in Renal Disease (MDRD) equation, S_f slope of the accelerated (fast: f) part of the blood activity clearance curve, S_s slope of the slower (s) part of blood activity clearance curve

consistent with rapid clearance of ^{123}I-MIBG from the blood and uptake into organs (such as the heart) by means of the norepinephrine transporter.

As intravascular activity appears to play no role in the variation of the counts measured in the mediastinum, those counts likely reflect a combination of mediastinal tissue activity and scatter from ^{123}I-MIBG in adjacent organs (e.g., liver, lungs) [13]. This shows that for routine quantification, the mediastinum is acceptable as a reference region. However, these findings do not confirm that the mediastinum represents a background region with only nonspecific uptake/binding. To test this hypothesis would require a study where the specific uptake of ^{123}I-MIBG via the presynaptic norepinephrine transporter (i.e., uptake 1) was blocked and compared to a similar study without blocking. To our knowledge this type of study has not been performed in humans.

In subjects with normal renal function, intravenously administered ^{123}I-MIBG is almost exclusively excreted via the kidneys within 24 h after injection, with approximately 35% of administered ^{123}I-MIBG already excreted by 6 h [5, 6]. There are complex interactions between sympathetic regulation of renal function and cardiac function. For example, increased sympathetic activity reduces the filtration fraction [14, 15]. In addition, renal dysfunction is often present in HF patients, which may further increase the interindividual variation of blood pool clearance [7, 8]. Moreover, as a reduced GFR is associated with a reduced blood clearance of ^{123}I-MIBG, the excretion of ^{123}I-MIBG is not only dependent on filtration but also by tubular secretion [16]. In the present study, although approximately 40% of the patients had decreased renal function, differences in the rate of renal excretion did not contribute to variability in the mediastinal and myocardial ^{123}I-MIBG uptake. Therefore, within the typical time frame of ^{123}I-MIBG cardiac imaging (up to 4 h after injection), ^{123}I-MIBG mediastinal and myocardial activity determinations appear independent of the rate of blood clearance via the kidneys.

Radioactivity as measured in the blood samples may be in part explained by ^{123}I not bound to MIBG and this may have influenced our results. However, according to specifications of the manufacturer the radiochemical purity of the ^{123}I-MIBG used prior to injection is always more than 97% and in clinical practice the fraction of free ^{123}I does not exceed 2%. Secondly, after intravenous administration, ^{123}I-MIBG in humans is very stable and not subject to in vivo deiodination [17]. In addition, the clearance rate of both ^{123}I-MIBG and free ^{123}I from the blood pool is rapid and is almost exclusively dependent on renal excretion. Therefore, the impact of free ^{123}I on the present results should be negligible.

In conclusion, in patients with ischemic heart disease, due to rapid clearance of ^{123}I-MIBG from the blood, the heart and mediastinal count densities measured on planar ^{123}I-MIBG images at 15 min and 4 h are not affected by residual vascular activity. In addition, this observation holds for the broad range of renal function commonly encountered in heart disease patients. Therefore, no correction for blood pool activity or renal function is needed for the calculation of myocardial WO. However, the clinical appropriateness of using mediastinal activity as a background correction in such calculations, which depend on the assumption that there is no specific uptake/binding in this region, remains to be demonstrated.

Conflicts of interest Arnold F. Jacobson is employed by GE Healthcare. None of the other authors have a conflict of interest to disclose. Grant support: none of the authors has been supported by a grant.

References

1. Cohn JN, Levine TB, Olivari MT, Garberg V, Lura D, Francis GS, et al. Plasma norepinephrine as a guide to prognosis in patients with chronic congestive heart failure. N Engl J Med 1984;311:819–23.
2. Verberne HJ, Brewster LM, Somsen GA, van Eck-Smit BL. Prognostic value of myocardial 123I-metaiodobenzylguanidine (MIBG) parameters in patients with heart failure: a systematic review. Eur Heart J 2008;29:1147–59.
3. Agostini D, Verberne HJ, Burchert W, Knuuti J, Povinec P, Sambuceti G, et al. I-123-mIBG myocardial imaging for assessment of risk for a major cardiac event in heart failure patients: insights from a retrospective European multicenter study. Eur J Nucl Med Mol Imaging 2008;35:535–46.
4. Jacobson AF, Senior R, Cerqueira MD, Wong ND, Thomas GS, Lopez VA, et al. Myocardial iodine-123 meta-iodobenzylguanidine imaging and cardiac events in heart failure. Results of the prospective ADMIRE-HF (AdreView Myocardial Imaging for Risk Evaluation in Heart Failure) study. J Am Coll Cardiol 2010;55:2212–21.
5. Kline RC, Swanson DP, Wieland DM, Thrall JH, Gross MD, Pitt B, et al. Myocardial imaging in man with I-123 meta-iodobenzylguanidine. J Nucl Med 1981;22:129–32.
6. Verberne HJ, Busemann Sokole E, van Moerkerken A, Deeterink J, Ensing G, Stabin M, et al. Clinical performance and radiation dosimetry of no-carrier-added vs carrier-added 123I-metaiodobenzylguanidine (MIBG) for the assessment of cardiac sympathetic nerve activity. Eur J Nucl Med Mol Imaging 2008;35:798–807.
7. Aaronson KD, Schwartz JS, Chen TM, Wong KL, Goin JE, Mancini DM. Development and prospective validation of a clinical index to predict survival in ambulatory patients referred for cardiac transplant evaluation. Circulation 1997;95:2660–7.
8. Flack JM, Neaton JD, Daniels B, Esunge P. Ethnicity and renal disease: lessons from the Multiple Risk Factor Intervention Trial and the Treatment of Mild Hypertension Study. Am J Kidney Dis 1993;21:31–40.
9. Bax JJ, Kraft O, Buxton AE, Fjeld JG, Parízek P, Agostini D, et al. 123I-mIBG scintigraphy to predict inducibility of ventricular arrhythmias on cardiac electrophysiology testing: a prospective multicenter pilot study. Circ Cardiovasc Imaging 2008;1:131–40.
10. Cockcroft DW, Gault MH. Prediction of creatinine clearance from serum creatinine. Nephron 1976;16:31–41.
11. Levey AS, Bosch JP, Lewis JB, Greene T, Rogers N, Roth D. A more accurate method to estimate glomerular filtration rate from serum creatinine: a new prediction equation. Modification of Diet in Renal Disease Study Group. Ann Intern Med 1999;130:461–70.
12. Tomson C, Blades S, Burden R, Cunningham J, Dennis J, Gilbert D, et al. Chronic kidney disease in adults. In: UK guidelines for identification, management and referral. 2009. Available at: http://www.renal.org/CKDguide/full/CKDprintedfullguide.pdf. Accessed 26 Jan 2011.
13. Verberne HJ, Somsen GA, Povinec P, van Eck-Smit BL, Jacobson AF. Impact of mediastinal, liver and lung (123)I-metaiodobenzylguanidine ((123)I-MIBG) washout on calculated (123)I-MIBG myocardial washout. Eur J Nucl Med Mol Imaging 2009;36:1322–8.
14. DiBona GF, Kopp UC. Neural control of renal function. Physiol Rev 1997;77:75–197.
15. Kon V, Yared A, Ichikawa I. Role of renal sympathetic nerves in mediating hypoperfusion of renal cortical microcirculation in experimental congestive heart failure and acute extracellular fluid volume depletion. J Clin Invest 1985;76:1913–20.
16. Blake GM, Lewington VJ, Zivanovic MA, Ackery DM. Glomerular filtration rate and the kinetics of 123I-metaiodobenzylguanidine. Eur J Nucl Med 1989;15:618–23.
17. Wafelman AR, Hoefnagel CA, Maessen HJ, Maes RA, Beijnen JH. Renal excretion of iodine-131 labelled meta-iodobenzylguanidine and metabolites after therapeutic doses in patients suffering from different neural crest-derived tumours. Eur J Nucl Med 1997;24:544–52.